



HAL
open science

Smart brute-force approach for distribution feeder reconfiguration problem

Guillaume Parlier, Hervé Guéguen, Feihu Hu

► **To cite this version:**

Guillaume Parlier, Hervé Guéguen, Feihu Hu. Smart brute-force approach for distribution feeder reconfiguration problem. *Electric Power Systems Research*, 2019, 174, pp.105837. 10.1016/j.epsr.2019.04.015 . hal-02161024

HAL Id: hal-02161024

<https://univ-rennes.hal.science/hal-02161024v1>

Submitted on 22 Oct 2021

HAL is a multi-disciplinary open access archive for the deposit and dissemination of scientific research documents, whether they are published or not. The documents may come from teaching and research institutions in France or abroad, or from public or private research centers.

L'archive ouverte pluridisciplinaire **HAL**, est destinée au dépôt et à la diffusion de documents scientifiques de niveau recherche, publiés ou non, émanant des établissements d'enseignement et de recherche français ou étrangers, des laboratoires publics ou privés.



Distributed under a Creative Commons Attribution - NonCommercial 4.0 International License

Smart brute-force approach for distribution feeder reconfiguration problem

Guillaume Parlier^{a,b}, Hervé Guéguen^{a,*}, Hu Feihu^b

^a*IETR CentraleSupélec, Rennes, France*

^b*School of Electrical Engineering, Xi'an Jiatong University, Xi'an, PR China*

Abstract

The massive introduction of generation at the distribution level changes the electric network operation paradigm. According to the rules that govern the relationship between the distribution system operator and the transmission system operator, it becomes interesting to reconfigure the distribution system to control the power consumption and injection at each substation and to determine the switch configuration that optimizes this behaviour at substations. This paper proposes a method to solve this distribution feeder reconfiguration (DFR) problem. First, an offline computation, based on a graph-oriented approach, finds all valid radial configurations and their similarities, then, according to a load setting, a sub approximation of the operating cost is computed and used with electrical constraints detection to reduce the number of necessary load flow computations in a brute-force approach to choose the optimal configuration. This method is exemplified on a test case including 4 substations, 124 nodes, 115 uncontrolled lines and 23 switch controlled lines.

Keywords: Automation, Smart Grids, Distribution feeder reconfiguration

1. Introduction

The massive introduction of renewable power generators in the distribution network changes the electric network operation paradigm: the power is not produced anymore only at transmission level, but the production is decentralized all over the grid. Consumptions at substations, connecting the distribution grid to the transmission one, then depend on consumption of loads and distributed generation and it may occur that power flows from distribution to transmission grid.

The distribution network is made of a group of interconnected electric radial circuits connected together by a set of switches and to the transmission grid by a set of substations. The operating cost of this distribution grid is related to the power consumption at each substation according to its power subscription, power losses in the lines and distributed power injected into the transmission system. This cost then depends on the configuration of the distribution grid and to optimize it the distribution system operator (DSO) should select the best configuration in order to control the substation consumption according to their subscription and to minimize power injection into the transmission system. This distribution feeder reconfiguration (DFR) then consists in choosing a topology of the network that minimizes the operating cost and connect all the nodes of the electric

*Corresponding author, CentraleSupélec, CS 47601, 35576 Cesson-Sévigné cedex, France

Email addresses: guillaumeparlier@gmail.com (Guillaume Parlier), herve.gueguen@centralesupelec.fr (Hervé Guéguen), hufeihu@xjtu.edu.cn (Hu Feihu)

grid to a substation by a tree satisfying the operating electrical constraints at node voltage and link current.

This DFR problem is a huge, non-linear integer problem. There is no easy solution to solve it, so many approaches that include some a priori knowledge on the problem and the objective function are proposed (Abbasi and Mehmood, 2014). These approaches may be classified (see e.g. (Tang et al., 2014) or (Ma et al., 2017)) according to the objective of DFR such as loss reduction, load balancing, voltage profile improvement, service restoration, or reliability improvement but also according to the optimization method such as heuristic methods (Kaveh et al., 2018; Pegado et al., 2019) or mixed integer programming (Zhai et al., 2018; Home-Ortiz et al., 2019). For all approaches, the most difficult point is to formalize the radiality constraint that ensures that each node is connected to one sub-station by a tree (Lavorato et al., 2012; Ahmadi and Marti, 2015). So, even for approaches based on heuristic methods that are quite popular, pre-processing of potential solutions in order to take into account only radial configurations is advocated (Andervazh et al., 2013; Possemato et al., 2015; Huang and Dinavahi, 2018). The number of switch configurations that define radial topologies is indeed much smaller than the global number of configurations. Moreover, some similarities among configurations can be used to detect and delete configurations that do not satisfy electrical constraints. Therefore, the number of eligible configurations may be heavily reduced.

In this paper, we present a methodology to solve the DFR problem when several substations are considered and the distribution system operating cost is based on subscription of substations and generation losses. This approach is based on the computation of all valid radial configurations of the distribution system. Then, considering that the most important part of the operating cost is related to substations and that load flow computation is the most time consuming, a sub approximation is used to rank the configurations. Finally, load flow computations are used to get the exact cost and check the satisfaction of electrical constraints. This approach makes it possible to find the optimal solution with few load flow computations, leading to a smart brute-force approach. In section 2, the optimization problem is described. Then in section 3, the computation of the set of radial configurations based on a graph approach is introduced. Finally, section 4 presents the optimization process and section 5 illustrates the effectiveness of the method on a test case including 4 sub-stations, 124 nodes, 115 uncontrolled lines and 23 switch controlled lines.

2. Description of the problem

Usually the cost paid by the distribution system operator (DSO) to the transmission system operator (TSO) is related to the power consumption at each substation (high to medium voltage) of the grid and can be divided in two parts: the power transit cost and the overconsumption cost. In this section, the chosen cost function is presented, then the parameters of the optimization problem are introduced and finally the operating constraints are given.

2.1. Cost function

The cost chosen in our optimization problem is based on the documentation of RTE, the French TSO (RTE, 2010). The variable part of the cost paid by the distributor depends on the subscription at each substation and can be divided in two sub costs.

Power transit cost. For a power subscription of a substation $P_{subscribed}$ (in kW), the cost associated to the consumption of an energy $E_{consumed}$ (in kW.h) during a period dt (in hours) is:

$$CS = \frac{dt}{8760} * b * \left(\frac{E_{consumed}}{dt * P_{subscribed}} \right)^c * P_{subscribed}$$

Where b in €/kW.year) and c are application dependent parameters. $E_{consumed}$ corresponds to the electric consumption at the substation and is null if energy is injected into the transmission system by the substation.

Overconsumption. When the average, over a ten-minute period, of the energy consumption of a substation is higher than that of the subscription, there is overconsumption that results in a cost. Thus, ΔP representing the positive difference between the average consumption and the subscription for a 10-minute period, the cost of overconsumption is described as follows:

$$CMDPS = \alpha * \sum_{dt} \Delta P$$

Where α is expressed in €/kW.

The global cost for a given period of time dt is then defined as follows:

$$J(X) = \sum_{substations} \underbrace{\frac{dt}{8760} * b * \left(\frac{E_{consumed}}{dt * P_{subscribed}} \right)^c * P_{subscribed}}_{\text{Power transit cost}} + \underbrace{\alpha * \sum_{dt} \Delta P}_{\text{Overconsumption cost}} \quad (1)$$

cost for each substation

2.2. Constraints

For the operation of the distribution network, two kinds of constraints can be identified.

Topological constraints. In order to operate the network, each node must be connected to a single substation and there must be no loop in the network, thus defining the *radiality constraint*.

Electrical constraints. The voltage at each node must not exceed 10% of the reference voltage and must not be less than 90% of it and the current in each line cannot exceed the ampacity of the line.

2.3. Problem setting

Considering a distribution system modelled by a graph with n nodes, $n_{substation}$ substations associated with their subscriptions, n_{link} uncontrollable links that are always connected, n_{switch} controllable switches that can be closed or open, a specific setting of consumption or generation at each node and a given time period dt , the problem is then to find the switch configuration that minimizes the cost $J(X)$ in (1) while satisfying the topological and electrical constraints.

To determine this optimal configuration, it is then necessary to compute the power consumption of each substation, to evaluate the cost function, and the voltage and current in the network to check that constraints are satisfied. Solving a power flow problem is therefore mandatory. As for a grid with n_{switch} switches that can be opened or closed, there are $2^{n_{switch}}$ possible configurations, the same number of power flow computations may be required in a brute-force approach. This leads to an unacceptable computation time. In addition, most of these configurations do not satisfy the radiality constraint. It is therefore interesting to determine the set of valid configurations to improve the effectiveness of the computation.

3. Computation of the admissible set of configurations

It is useless to try to calculate the cost (and then the power flow) associated with a configuration that does not satisfy the radiality constraint. The first step is therefore to determine all configurations of switches that satisfy this constraint. This is based on the notion of trees in graph theory.

3.1. Prerequisites

For an electrical grid the radiality constraint is satisfied when each node is connected to one and only one substation by only one path then defining trees from each substation. Some general properties of trees are then useful.

Number of edges in a tree. In a tree with v vertices the total number of edges is $v - 1$.

Opening of an edge in a tree. In a tree, when an edge is removed two trees are created.

Connection of two trees. If an edge is created between two nodes of two trees, a new tree is created.

Number of trees. In a graph with v vertices, to form n_g trees $v - n_g$ edges are necessary

3.2. Higher bound of the number of radial configurations

To satisfy, the radiality constraint, $n_{substation}$ trees must be built, so $(n + n_{substation}) - n_{substation} = n$ edges must be closed in the network. Since among these n edges n_{link} cannot be changed, $n - n_{link}$ switches must be closed.

Thus the maximum number of radial configurations in a distribution network is $\binom{n_{switch}}{n - n_{link}}$; $(n - n_{link})$ switches must be chosen among the n_{switch} switches that can be closed.

The total number of radial configurations is much smaller than this total number of configurations, thus a method that find all radial configurations, rather than considering random configurations, is presented in the following sub sections.

3.3. Abstract graph

The purpose of this section is to show how to build a graph that will make it easier to find the radial configurations of the initial graph. This new graph is such that all its tree configurations correspond to all radial configurations of the initial network. The approach is based on the assumption that in the initial graph, when all switches are open, all connected sub graphs are trees and no substation is connected to another one.

Building of new graph. The method to obtain the abstract graph from the initial graph that satisfies the required properties is then:

1. *Opening of all switches:* All the switches of the initial grid are opened,
2. *Creation of a virtual path:* In the grid with open switches, virtual links connecting all substations are added.
3. *Equivalent nodes:* All the nodes that are connected to each other are equivalent. Cosets define the vertices of the abstract graph.
4. *Edges of the abstract graph:* Each switch defines an edge linking the cosets of the original nodes. This may lead to define edges linking the same abstract nodes. The edges that define self-loop from one node to itself are removed and the corresponding switch must remain open. Two different edges that link the same abstract nodes are merged.

We can check that this procedure transforms each radial configuration of the initial graph into a tree of the abstracted graph. Indeed, for each radial configuration if the substations are connected by a virtual link this defines a tree (connection property). When the equivalent nodes are merged this still defines a tree in the abstract graph. In the same way, if we consider a tree in the abstract graph, this is equivalent to connect trees of the initial graph as all equivalent nodes are one tree. So, a tree of the initial graph is defined and when the virtual link is not considered a radial configuration of the initial graph is obtained.

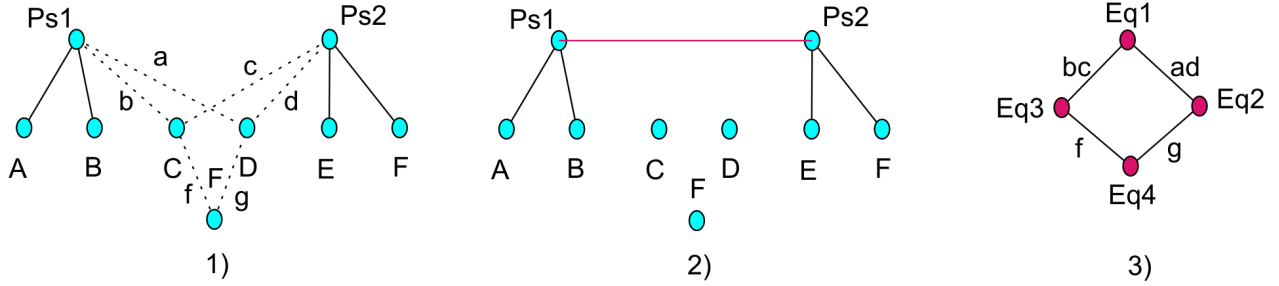


Figure 1: Example of the building process of the abstract graph

This graph transformation method is illustrated in figure 1. The original graph (see figure 1.1) is made of two substations (PS1 and PS2) and seven electric nodes. To connect all points of the electric system there are physical lines (plain lines) and switchable lines (dotted lines). At the first step of the method, the substations are connected to each other and the switches are open leading to graph 1.2. For this modified graph, table 1 specifies the equivalent nodes and the switches are considered to build the edges leading to the final abstract graph (1.3).

Coset	nodes
Eq1	PS1 PS2 A B E F
Eq2	D
Eq3	C
Eq4	G

Table 1: Equivalent nodes of the initial graph

On this graph, when the switches a, f and g are closed a tree is obtained, thus defining a tree in the original graph.

The second step of the approach then defines all tree configurations for this type of graphs where all edges are controllable.

3.4. Fundamental Cutset Method

Mayeda and Seshu (1965) introduced the fundamental cutset method that makes it possible to find all the trees of a graph in which all edges are switches. It can then be applied on the equivalent graph that was built in the previous section. This paper will not detail the method and readers should refer to Mayeda and Seshu (1965) for a complete presentation, but the example in figure 2 will be used to present the iterative process.

This method is based on the notion of *fundamental cutset* that is, considering a spanning tree T built from a graph G and an edge e in T , the set (denoted $S(T, e)$) of edges in G that connect the

two sub-trees that are generated when the edge e is removed from T . For example, in figure 2 for graph G if the tree T_0 and the edge d are considered, the fundamental cutset is $S(T_0, d) = \{f, g, i\}$.

The first step in this method is to generate a first tree from the graph and then to order the edges of this tree in order to be able to generate all trees but only once. In the example, the tree T_0 is selected and the edges $E_{T_0} = \{a, b, c, d, e\}$ are ordered in alphabetical order.

In the second step, each edge of the initial tree is considered, that is:

1. the edge is removed from the tree,
2. the fundamental cutset associated with this edge and the initial tree T_0 is computed,
3. each edge of the fundamental cutset is considered to generate a new tree; for example, in figure 2 from T_0 , considering $S(T_0, d) = \{f, g, i\}$, it is possible to generate the three trees T_{41} , T_{42} and T_{43} .

Then for each of these new trees T_i the process is iterated. For each edge of the initial tree T_0 that is after (according to the order relationship initially defined) the edge that was removed to generate the considered tree T_i , the process is then:

1. the edge is removed from the tree; in the example, from T_{41} , T_{42} and T_{43} the only edge that has to be considered is e because of the order relationship introduced on E_{T_0} ;
2. the fundamental cutsets associated with this edge and the trees T_0 and T_i are computed; for example $S(T_0, e) = \{i, h\}$ and $S(T_{42}, e) = \{d, f, g, h\}$;
3. each edge in the intersection of these fundamental cutsets is considered to generate a new tree; in the example, from T_{42} , only edge h can be used to generate T_{421} .

When in all branches all required edges has been considered, the building of all possible configurations is finished. It is then easy to come back to the original graph by considering equivalent nodes and merged switches.

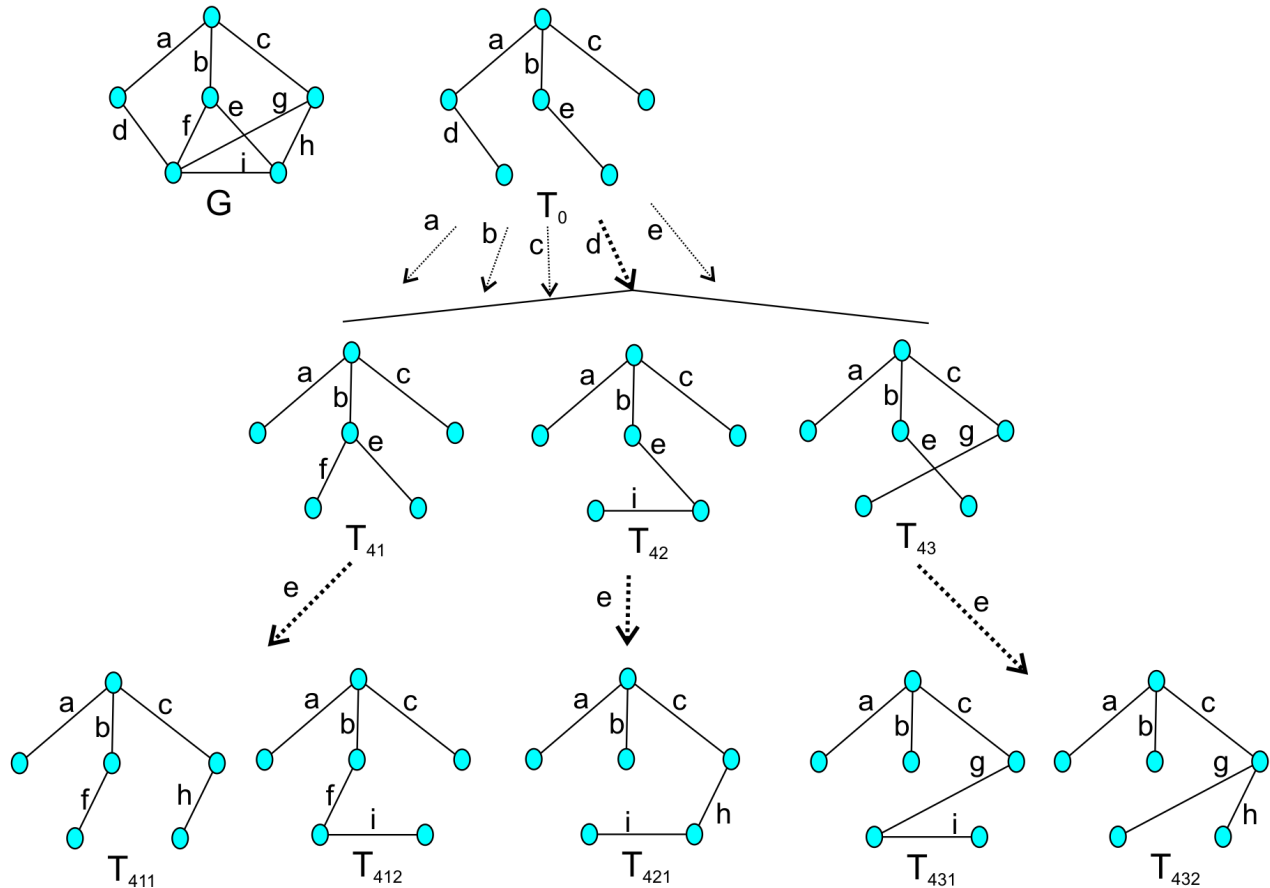


Figure 2: Fundamental cutset method

4. Search of the best configuration

The work of section 3 reduces the size of the set of admissible configurations and a brute-force approach can be used. However the computation of the cost for each configuration is still time expensive because of the power flow computation. Two ideas are used to minimize the number of these computations:

- computation of a sub approximation of the cost for each configuration,
- reducing the number of admissible configurations by detection of electrical constraint violation.

4.1. Sub approximation of the cost

Since the exact calculation of costs is an expensive step (due to the power flow computations), a cost approximation can be used. The cost function is, in fact, an increasing function of power at each substation, so with a lower approximation of power consumption at each substation, a sub approximation of the total cost can be found. The total power consumption of a substation is described by $S_{substation} = \sum S_i + Pl$ where S_i characterizes the consumption of each node connected to this substation by a tree and Pl the line losses. Since the transfer of power from the distribution grid to the transmission grid has no value, $S_{substation}$ may be considered as positive for cost computation. Since line losses consume power in the network, $S_{substation} \geq \sum S_i$ then $\sum S_i$ is a lower

approximation of the consumption that can also be considered as positive for cost computation and that can be used to compute a lower approximation of the cost at each substation.

4.2. Identification of impossible configurations

Two configurations can share common tree parts. If an electrical constraint is not satisfied in this part in the first configuration, it is also not satisfied in the second one. These configurations are then considered as similar and can be identified by a graph approach.

Branch of the grid. The branch of a tree T including node k connected to the substation l is the sub-graph made of the substation l and the nodes connected to k without passing through the substation l . Similarly, the branch associated to a link kn is the branch associated to the nodes k and n . For example, for the network described in figure 3.1, with 9 nodes (A to I) and two substations PS1 and PS2, the branch associated to H is made of the nodes A, D, E, H and the substation PS1 and the branch associated to link FI is made of nodes B, F, I and substation PS1.

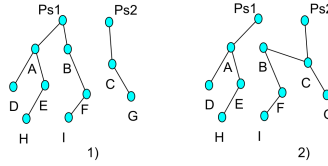


Figure 3: Branches and configuration similarities

Since the voltage at the substation is considered as fixed, the power flow in one branch does not depend on the other branches of the tree. Therefore, if an electrical constraint is not satisfied in a configuration that defines a branch it is not satisfied in all configurations that define the same branch. For example, if a constraint is violated at node A in figure 3.1, it is also violated in the configuration of figure 3.2.

Thus, when the power flow computation detects an electrical constraint in one configuration, the set of configurations that do not satisfy the same electric constraint can be identified by the following method:

- the branch of the constrained node or link is identified,
- all the switches connected to one node of the branch and their states (open or closed) are identified,
- all the radial configurations that have these switches in the same state are similar and do not satisfy the same electric constraint.

4.3. Optimization Method

In order to find the optimal solution the following method, based on these ideas, is then applied:

Initialization. A sub approximation of the cost for all radial configurations is computed as stated in sub-section 4.1; then all these configurations are ranked in ascending order of the sub approximation.

For the first configuration (lowest sub approximation), the cost of the configuration is computed with a power flow computation. If it does not satisfy electrical constraints, the cost is infinite and the similar configurations are removed. The cost of the configuration is stored as optimal.

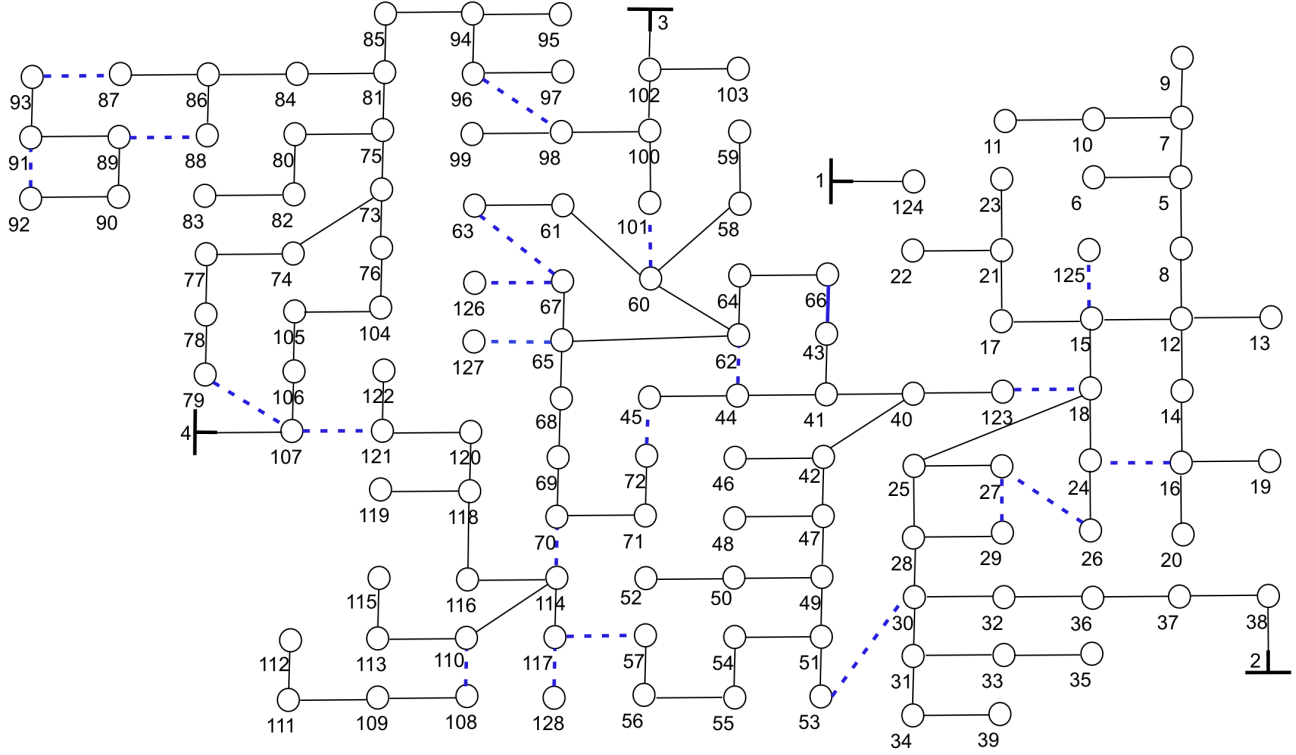


Figure 4: 124 nodes grid

Iteration process. If the sub approximation of the cost of the next configuration is higher than the minimum real cost, the optimal configuration has been found and the process stops. If not, the real cost of the configuration is computed, the optimal configuration and cost are modified if the cost is improved or the similar configurations are removed if needed.

This method gives an exact solution of the DFR problem and through the graph oriented pre analysis, the number of power flow computations is greatly reduced.

5. Application on a 124 nodes grid

5.1. Presentation of the example

In this section, the method introduced in section 4 is applied on a test grid presented in figure 4. This test network is a 124 nodes network with 4 substations, 115 physical links between the nodes (plain lines) and 23 switches (dotted lines). The load (consumption or generation) of each node, the power subscription of each substation and the parameters of the PI model of the lines are specified in Appendix A. The time dt used to compute criterion (1) is 1 hour and the parameters are $b = 79.74 \text{ €/kW/year}$, $c = 0.8$ and $\alpha = 1.6568 \text{ €/kW}$.

In order to compute the cost of the configuration the backward-forward method introduced in Shirmohammadi et al. (1988) is used for power flow computations.

5.2. Computation of the abstract grid

For this grid, the first step of abstraction, described in section 3, leads to the graph represented in figure 5 with 10 cosets and 12 edges that are detailed in Appendix B. It can be seen in table B.6 that some switches are not associated with any edge of this abstract graph which means that they should remain open in all radial configurations.

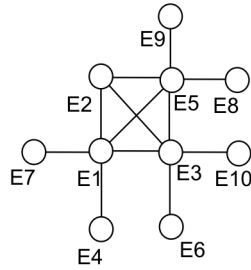


Figure 5: 124 nodes grid abstract model

The application of the cutset method described in sub-section 3.4 then determines $\binom{6}{3} = 20$ tree configurations for the abstract graph. This number is consistent with the fact that some edges (e.g. $E1E7$) belong to all valid configurations. These 20 tree configurations correspond to 92 radial configurations for the original grid. As each configuration is specified by 9 closed switches this number is to compare to $\binom{23}{9} = 817190$ that first appears as the upper bound of the number of configurations. This highlights the importance of the reduction method in order to apply a brute-force approach to the problem.

5.3. Cost computation

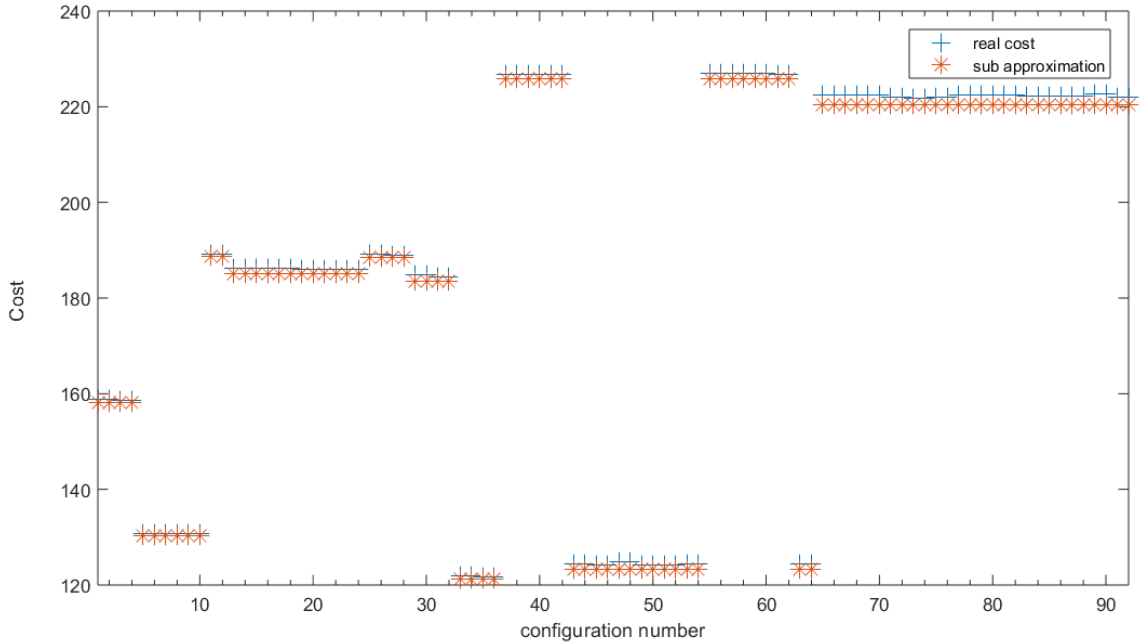


Figure 6: Costs of all radial configurations and their sub approximation

In order to assess our method, the real costs of all radial configurations and their sub approximations computed according to sub-section 4.1 are given in figure 6. It can be seen that the sub approximation gives a good approximation of the real cost. However, it is not sufficient to determine the optimal configuration as the electric constraint satisfaction is not checked.

When the method described in section 4 is applied, the real costs of only 4 configurations (33, 34, 35 and 36 that have the same sub approximation, see figure 6) are computed, and the configuration 35 is chosen as the optimal one.

6. Conclusion

In this paper, a method that gives an exact solution to the considered DFR problem in a reasonable computation time is presented. Even if the DFR problem is huge, a smart brute-force approach is made possible thanks to the reduction of the size of the problem based on a graph theory pre-processing. This reduction method finds all the configurations that satisfy the radiality constraint. This computation only depends on the grid topology and not on the loads, it can then be done only once for each grid. From the reduced valid configuration set and the loads, it is possible to compute a sub approximation of the cost and then use it to reduce the number of power flow computations. Finally, the analysis of configurations that do not satisfy electrical constraints also reduces this number. The offline pre-processing and the considerations that are introduced, greatly reduce the calculations that have to be done online. It is thus possible to consider the introduction of this approach for the actual operation of a distribution network.

Future works will consider two other aspects of this DFR: the uncertainty and the variability of the loads. As it can be seen in the example many configurations may have an equivalent cost for a given load setting, but these loads are not exactly known and this uncertainty may have a huge effect, for example, when the optimal configuration is closed to electrical constraints. The first challenge is then to consider the robustness of the optimality of the configuration when introducing loads uncertainties. The second one is that during one day the loads change and then the optimal configuration also changes. However, the daily number of configuration switching is limited, then the choice of the optimal configuration at one time step must depend on the future or at least on its prediction, this dynamical aspect has then to be introduced in the process.

Appendix A. Test case data

This appendix details the characteristic of the test case that was considered. The 4 substations are the first 4 nodes of the graph. The power subscription for the 4 substations are: 150kW, 200kW, 250kW and 90kW.

The parameters of the lines are : $Z_{lin} = 2 + 0.5 * i \Omega/m$ and $C_{lin} = 3 * 10^{-6} F/m$

Table A.2 contains the characteristics of the uncontrollable links of the network. The *Nodes* column specifies the number of the nodes that are connected and the *Length* column the length of the corresponding line. The switches are described in table A.3. Each switch is identified by a number in *swit.* column and associated with the nodes and the length of the line that it controls. In these tables, the length of the lines are given in meters.

The power consumption of each node is given in table A.4

Appendix B. Detailed results

In order to apply the smart-brute force approach to solve the problem, all radial configurations are considered. The first step of the method presented in section 3 then leads to determine the cosets of nodes that are detailed in table B.5 and the set of edges that are given with their associated switches in table B.6. As 10 nodes are built in the abstract graph, 9 switches (among the 23) should be chosen to get all the radial configurations. The second step finds 92 different radial

Nodes	Length	Nodes	Length	Nodes	Length	Nodes	Length
1-124	88.2	30-31	105	60-61	82.5	89-90	75
2-38	36.6	30-32	60	60-62	105	89-91	202.5
3-102	178.2	31-33	82.5	61-63	82.5	90-92	75
4-107	39.6	31-34	67.5	62-64	75	91-93	142.5
5-6	52.5	32-36	90	62-65	225	94-95	52.5
5-7	75	33-35	150	64-66	75	94-96	82.5
5-8	90	34-39	90	65-67	165	96-97	676.5
7-9	60	36-37	105	65-68	75	98-99	90
7-10	97.5	37-38	60	68-69	52.5	98-100	67.5
8-12	60	40-41	195	69-70	105	100-101	82.5
10-11	75	40-42	75	70-71	127.5	100-102	90
12-13	67.5	40-123	112.5	71-72	97.5	102-103	60
12-14	67.5	41-43	90	73-74	60	104-105	165
12-15	90	41-44	75	73-75	82.5	105-106	90
14-16	127.5	42-46	97.5	73-76	75	106-107	240
15-17	45	42-47	75	74-77	82.5	108-109	67.5
15-18	247.5	44-45	97.5	75-80	82.5	109-111	97.5
16-19	75	47-48	150	75-81	60	110-113	67.5
16-20	75	47-49	60	76-104	82.5	110-114	97.5
17-21	30	49-50	60	77-78	97.5	111-112	210
18-24	75	49-51	75	78-79	82.5	113-115	172.5
18-25	90	50-52	90	80-82	105	114-116	135
21-22	112.5	51-53	45	81-84	120	114-117	300
21-23	105	51-54	75	81-85	210	116-118	90
24-26	97.5	54-55	75	82-83	120	118-119	172.5
25-27	157.5	55-56	75	84-86	30	118-120	37.5
25-28	75	56-57	150	85-94	135	120-121	157.5
28-29	165	58-59	60	86-87	67.5	121-122	97.5
28-30	82.5	59-60	37.5	86-88	142.5		

Table A.2: Uncontrollable links: connected nodes and length

Swit.	Nodes	Length	Swit.	Nodes	Length
1	15 - 125	231.6	13	65 - 127	76.8
2	16 - 24	59.1	14	67 - 126	153
3	18 - 123	136.2	15	70 - 114	206.7
4	26 - 27	144.9	16	79 - 107	71.1
5	27 - 29	231.6	17	87 - 93	81
6	30 - 53	217.2	18	88 - 89	103.8
7	43 - 66	61.2	19	91 - 92	129.3
8	44 - 62	82.8	20	96 - 98	159.3
9	45 - 72	177	21	107 - 121	103.5
10	57 - 117	83.4	22	108 - 110	225.3
11	60 - 101	101.4	23	117 - 128	187.8
12	63 - 67	84			

Table A.3: Switches: connected nodes and length of the associated lines

Node	P	Q	Node	P	Q	Node	P	Q
5	1000	18700	47	-3800	12500	88	23400	6100
6	1300	25900	48	17800	7100	89	5600	4400
7	23100	5600	49	23500	19300	90	-4400	400
8	9900	17800	50	4400	8200	91	-6600	7200
9	23400	14400	51	5400	21000	92	300	1900
10	13000	3000	52	19400	7200	93	7000	-5300
11	8300	18600	53	17800	27900	94	9800	18300
12	25400	18900	54	21400	18200	95	-300	21400
13	-9300	17000	55	-5700	5600	96	-7100	5700
14	7500	7500	56	13600	8400	97	-9900	-1200
15	-5400	22600	57	-8000	-900	98	-10000	-2500
16	3000	-200	58	23400	-9400	99	-4300	700
17	3700	5000	59	24600	-6900	100	-3000	-4500
18	11900	12500	60	16800	10000	101	14000	26100
19	5800	5900	61	-1300	12900	102	27600	-1200
20	10600	16300	62	-5200	16900	103	9300	5000
21	28100	18900	63	14000	-7800	104	11000	600
22	6000	23300	64	-7800	-3900	105	-7300	7400
23	-4700	-7600	65	-9300	7400	106	-3100	-9000
24	-6700	-3500	66	23300	14700	107	28200	7200
25	3000	2000	67	10800	24600	108	28500	20500
26	-9600	11600	68	-6100	26400	109	-9800	17200
27	-6200	-4200	69	-5700	10700	110	18300	15800
28	15300	24400	70	-4300	12400	111	12100	-1300
29	29000	12800	71	-9900	20700	112	20900	-900
30	29900	12100	72	24000	26700	113	4800	25700
31	10600	3200	73	29500	10200	114	24300	6100
32	7200	9700	74	800	-6000	115	2700	14400
33	-7200	25500	75	10300	13400	116	26400	26400
34	-7500	7400	76	20500	-6700	117	13700	3300
35	23100	5800	77	16500	1070	118	24200	7700
36	14600	22800	78	-3200	27600	119	26200	-8700
37	25500	27300	79	13600	7600	120	11300	18700
38	-2400	300	80	27700	16300	121	-2900	3400
39	26000	13700	81	8100	23600	122	-2500	2900
40	10200	14500	82	11300	12200	123	6100	11900
41	22800	11300	83	17200	4700	124	-8100	12100
42	-1900	8200	84	-500	13200	125	1000	-400
43	7100	28700	85	24700	6300	126	-300	-3900
44	14800	17800	86	-5500	7700	127	28300	27500
45	18800	3900	87	2000	6000	128	22800	19200
46	10700	12300						

Table A.4: Nodal Load: active (P) and reactive (Q) power

Coset	Nodes
E1	1 2 3 4 102 103 100 101 98 99 9 7 10 11 5 6 23 8 22 21 17 15 12 13 34 31 30 28 25 18 14 39 33 32 29 27 24 16 19 35 36 26 20 37 38 104 105 106 107 76 77 78 79 73 74 75 80 82 83 81 84 86 87 85 88 94 96 95 97 124
E2	52 50 53 49 51 54 55 56 57 47 48 42 46 40 123 11 41 43 44 45
E3	110 113 115 112 114 116 118 119 117 120 121 122
E4	89 90 92 91 93
E5	58 59 60 61 63 62 65 68 64 67 69 66 70 71 72
E6	108 109 111 112
E7	125
E8	127
E9	126
E10	128

Table B.5: Abstract graph: cosets of nodes

Edge	Switches	Edge	Switches
E1E2	3 6	E2E5	7 8 9
E1E3	21	E3E5	15
E1E4	17 18	E3E6	22
E1E5	11	E3E10	23
E1E7	1	E5E8	13
E2E3	10	E5E9	14

Table B.6: Abstract graph: Correspondence between edges and switches

configurations of the initial graph that are detailed in table B.7. In this table, each configuration is identified by its number and associated to the switches that are closed knowing that switches 1, 13, 14, 22, and 23 should always be closed. It can be noticed that switches 2, 4, 5, 12, 16, 19, and 20 should always remain open.

Finally the computed cost (according to (1)) for each configuration is given in table B.8

References

- Abbasi, R. S., Mehmood, T., 2014. Feeder reconfiguration techniques: A review. In: 2014 International Conference on Energy Systems and Policies (ICESP). IEEE.
- Ahmadi, H., Marti, J. R., 2015. Mathematical representation of radiality constraint in distribution system reconfiguration problem. *International Journal of Electrical Power & Energy Systems* 64, 293 – 299.
- Andervazh, M., Olamaei, J., r. Haghifam, M., 2013. Adaptive multi-objective distribution network reconfiguration using multi-objective discrete particles swarm optimisation algorithm and graph theory. *IET Generation, Transmission & Distribution* 7 (12), 1367–1382.
- Home-Ortiz, J. M., Vargas, R., Macedo, L. H., Romero, R., 2019. Joint reconfiguration of feeders and allocation of capacitor banks in radial distribution systems considering voltage-dependent models. *International Journal of Electrical Power & Energy Systems* 107, 298 – 310.

Conf.	Swit.	Conf.	Swit.	Conf.	Swit.	Conf.	Swit.
1	3-11-17-21	24	6-9-18-21	47	9-11-17-10	70	3-9-18-10
2	3-11-18-21	25	3-15-17-21	48	9-11-18-10	71	6-7-17-10
3	6-11-17-21	26	3-15-18-21	49	7-11-17-15	72	6-7-18-10
4	6-11-18-21	27	6-15-17-21	50	7-11-18-15	73	6-8-17-10
5	7-11-17-21	28	6-15-18-21	51	8-11-17-15	74	6-8-18-10
6	7-11-17-21	29	3-11-17-10	52	8-11-18-15	75	6-9-17-10
7	8-11-18-21	30	3-11-18-10	53	9-11-17-15	76	6-9-18-10
8	8-11-18-21	31	6-11-17-10	54	9-11-18-15	77	3-7-17-15
9	9-11-17-21	32	6-11-18-10	55	10-7-17-21	78	3-7-18-15
10	9-11-18-21	33	3-11-17-15	56	10-7-18-21	79	3-8-17-15
11	10-11-17-21	34	3-11-18-15	57	10-8-17-21	80	3-8-18-15
12	10-11-18-21	35	6-11-17-15	58	10-8-18-21	81	3-9-17-15
13	3-7-17-21	36	6-11-18-15	59	10-9-17-21	82	3-9-18-15
14	3-7-18-21	37	7-15-17-21	60	10-9-18-21	83	6-7-17-15
15	3-8-17-21	38	7-15-18-21	61	10-15-17-21	84	6-7-18-15
16	3-8-18-21	39	8-15-17-21	62	10-15-18-21	85	6-8-17-15
17	3-9-17-21	40	8-15-18-21	63	10-11-17-15	86	6-8-18-15
18	3-9-18-21	41	9-15-17-21	64	10-11-18-15	87	6-9-17-15
19	6-7-17-21	42	9-15-18-21	65	3-7-17-10	88	6-9-18-15
20	6-7-18-21	43	7-11-17-10	66	3-7-18-10	89	3-15-17-10
21	6-8-17-21	44	7-11-18-10	67	3-8-17-10	90	3-15-18-10
22	6-8-18-21	45	8-11-17-10	68	3-8-18-10	91	6-15-17-10
23	6-9-17-21	46	8-11-18-10	69	3-9-17-10	92	6-15-18-10

Table B.7: Radial configurations: Closed switches

Conf.	Cost	Conf.	Cost	Conf.	Cost	Conf.	Cost
1	159.12	24	186.54	47	125.30	70	223.38
2	159.12	25	189.59	48	125.30	71	222.74
3	150.02	26	189.59	49	124.44	72	222.74
4	159.02	27	189.50	50	124.44	73	222.71
5	130.96	28	189.50	51	124.37	74	222.71
6	130.96	29	185.51	52	124.37	75	222.74
7	130.94	30	185.51	53	124.78	76	222.74
8	130.94	31	185.03	54	124.78	77	223.57
9	131.01	32	185.03	55	228.05	78	223.57
10	131.01	33	122.23	56	228.05	79	223.41
11	189.80	34	122.23	57	228.02	80	223.41
12	189.80	35	122.09	58	228.02	81	223.48
13	186.73	36	122.09	59	228.05	82	223.48
14	186.70	37	227.73	60	228.05	83	223.22
15	186.70	38	227.73	61	227.54	84	223.22
16	186.70	39	227.65	62	227.54	85	223.06
17	186.73	40	227.65	63	124.97	86	223.06
18	186.73	41	227.57	64	124.97	87	223.13
19	186.53	42	227.57	65	223.37	88	223.13
20	186.53	43	124.80	66	223.37	89	223.79
21	186.51	44	124.80	67	223.34	90	223.79
22	186.51	45	124.56	68	223.34	91	222.93
23	186.54	46	124.56	69	223.38	92	222.93

Table B.8: Radial configurations: cost in euro

- Huang, S., Dinavahi, V., July 2018. Fast distribution network reconfiguration with graph theory. *IET Generation, Transmission & Distribution* 12, 3286–3295(9).
- Kaveh, M. R., Hooshmand, R.-A., Madani, S. M., 2018. Simultaneous optimization of re-phasing, reconfiguration and DG placement in distribution networks using BF-SD algorithm. *Applied Soft Computing* 62, 1044 – 1055.
- Lavorato, M., Franco, J. F., Rider, M. J., Romero, R., 2012. Imposing radiality constraints in distribution system optimization problems. *IEEE Transactions on Power Systems* 27 (1), 172–180.
- Ma, Y., Liu, F., Zhou, X., Gao, Z., 2017. Overview on algorithms of distribution network reconfiguration. In: 2017 36th Chinese Control Conference (CCC). pp. 10657–10661.
- Mayeda, W., Seshu, S., 1965. Generation of trees without duplications. *IEEE Transactions on Circuit Theory* 12 (2), 181–185.
- Pegado, R., Naupari, Z., Molina, Y., Castillo, C., 2019. Radial distribution network reconfiguration for power losses reduction based on improved selective BPSO. *Electric Power Systems Research* 169, 206 – 213.
- Possemato, F., Paschero, M., Livi, L., Rizzi, A., Sadeghian, A., 2015. On the impact of topological properties of smart grids in power losses optimization problems. *International Journal of Electrical Power & Energy Systems* 78, 755 – 764.
- RTE, 2010. Comprendre le tarif, tarif d’utilisation du réseau public de transport d’électricité. Tech. rep., Réseau de Transport d’Electricité, RTE.
- Shirmohammadi, D., Hong, H. W., Semlyen, A., Luo, G. X., 1988. A compensation-based power flow method for weakly meshed distribution and transmission networks. *IEEE Transactions on Power Systems* 3 (2), 753–762.
- Tang, L., Yang, F., Ma, J., 2014. A survey on distribution system feeder reconfiguration: Objectives and solutions. In: 2014 IEEE Innovative Smart Grid Technologies - Asia (ISGT ASIA). pp. 62–67.
- Zhai, H., Yang, M., Chen, B., Kang, N., 2018. Dynamic reconfiguration of three-phase unbalanced distribution networks. *International Journal of Electrical Power & Energy Systems* 99, 1 – 10.